Desalination and Water Treatment
www.deswater.com

doi: 10.5004/dwt.2020.25026

179 (2020) 368–377
March

Effective decoloration of cationic dyes by silica gel prepared from Tunisian sands and TiO_2/silica gel composites: dual adsorption and photocatalytic processes

Khalil Lazaar[a,*], Walid Hajjaji[b,c], Robert C Pullar[d], Hajer Chargui[a], Bechir Moussi[a], João Labrincha[d], Fernando Rocha[c], Fakher Jamoussi[a]

[a]*Georessources Laboratory, CERTE, 273 - 8020 Soliman, Tunisia, Tel: +216 95 14 93 77; emails: lazaar.khalil@yahoo.fr (K. Lazaar), hajerchargui@gmail.com (H. Chargui), bechirmoussi2007@gmail.com (B. Moussi), fjamoussi@yahoo.com (F. Jamoussi)*
[b]*Natural Water Treatment Laboratory, CERTE, 273 - 8020 Soliman, Tunisia, email: w.hajjaji@ua.pt*
[c]*Geobiotec, Geosciences Department, University of Aveiro, 3810 - 193 Aveiro, Portugal, email: tavares.rocha@ua.pt*
[d]*Department of Materials and Ceramic Engineering/CICECO – Aveiro Institute of Materials, University of Aveiro, 3810 - 193 Aveiro, Portugal, emails: rpullar@ua.pt (R.C. Pullar), jal@ua.pt (J. Labrincha)*

Received 9 March 2019; Accepted 13 October 2019

ABSTRACT

Silica gels synthesized from Tunisian sands employed as alternative low-cost adsorbents, and silica gel/TiO_2 composites for combined absorption/photocatalytic decoloration of methylene blue (MB) dye solutions, were studied. The silica gel is characterized by a high specific surface area of up to194 m^2/g and is likely to increase in aqueous solution, according to the solid/liquid ratio which modulates the degree of hydration. This was determined at various synthesis pH values. For this silica gel, the maximum adsorption capacity (up to 91%, 125 mg/g) was obtained in acidic medium (pH 3). The adsorption mechanism fitted better using the Langmuir model, and the adsorption kinetics of the dye on these materials was well described by the second-order model. Silica gel/TiO_2 demonstrated an effective degradation of MB the first stage (30 min without UV-light exposure) and under UV. The kinetics of discoloration of MB followed a pseudo-first-order rate law. We can remark that 5 h of UV irradiation was enough to achieve 99% discoloration of the MB. The findings demonstrated the applicability of this silica gel/TiO_2 catalyst for the photocatalytic oxidation of MB.

Keywords: Silica gel; Titania; Cationic dye; Adsorption; Photocatalysis

1. Introduction

Currently, dyes play an important role in the industrial sector. These are used in the paper, cosmetics, food processing, pharmaceutical and especially in the textile industry. According to their chemical structure and method of application to the various substrates (textiles, paper, leather, plastics, etc.), there are different classes of dyes such as azo, reactive, acidic, basic, neutral, anthraquinone, disperse and direct. Azo and anthraquinone dyes are, however, the most used in the textile industry [1–3]. Azo dyes, in particular, are the most commonly used in the textile industry, such as methylene blue (MB = $C_{16}H_{18}ClN_3S$), which is a cationic dye. This dye poses a real danger when released into wastewater, since it may cause health issues such as burning eyes, and other harmful environmental effects such as blocking photosynthesis of waterborne flora [3–5]. The removal of this dye from wastewaters consists currently of distinct technological approaches, such as membrane filtration [6], coagulation–flocculation [7], chemical oxidation, electrochemical processes and adsorption [8,9]. The last one is a nondestructive process, by which the contaminants

* Corresponding author.

can be transferred from wastewater to an adsorbent [10,11]. Currently, photocatalytic decoloration is one of the most promising technologies for the removal of organic pollutants [12–14]. Titanium dioxide (TiO_2) is the common photocatalyst used [15] since it possesses interesting features such as high degradation efficiency, stability and low production cost [16–18].

Instead of using suspended photocatalytic particles, which must subsequently be removed/filtered from the treated water, the use of supported TiO_2/systems is very attractive. The use of silica gel as a substrate might assure high surface area, while it is hydrophobic and relatively cheap. Additionally, its high adsorption capacity might also contribute to the retention/immobilization of dye molecules [19,20]. Due to those properties, this material is widely used in fillers [21], coatings [22], catalyst supports and hygroscopic packaging for optical [23], electronic [24] and pharmaceutical [25] products.

Several studies have investigated the photocatalytic degradation of organic pollutants based on TiO_2 suspended in wastewater [26–31]. In this work, we study the dual effects of a silica gel absorbent produced from a natural resource as various pH values, and combined with a photocatalytic TiO_2 additive, on the removal of MB from water.

2. Materials and methods

2.1. Materials

The silica gel (GM) used in this study was prepared from Tunisian sands, which have been characterized in our previous work [5]. These materials were collected from the Fortuna formation in the North of Tunisia. The TiO_2 used was a commercial titania (Aeroxide P25, Evonik, Aveiro, Portugal).

2.2. Silica gel and silica gel/TiO_2 preparation

Silica gels were produced by Tunisian sand using three steps as proposed by Lazaar et al. [5]: (i) the preparation of sodium silicates, (ii) the dissolution, and (iii) the formation. The intermediate compound was obtained by heating at 1,060°C a mixture of sodium carbonate and silica sand (molar ratios $n = SiO_2/Na_2O$ equal to 1.5) [32,33]. 10 g of this prepared amorphous sodium silicate was dissolved in 500 ml of distilled water (at 160°C) with stirring for 10 min to obtain hydrated sodium silicate [32,34]. The final product (silica gel) was extracted after the dropwise addition of 2 M hydrochloric acid solution (pH 3), with washing to eliminate Cl^- ions [33,35], and drying for 24 h at 60°C. In this work, silica gels (GM) were prepared under different pH values (3, 6 and 10) from silicates, which were denoted as GM3, GM6, and GM10, respectively (Table 1).

TiO_2/silica gel mixtures were prepared by simply mixing the silica gel prepared at pH 3 (GM3) with a commercial titania (Aeroxide P25, Evonik, Aveiro, Portugal). The TiO_2/silica gel composites were synthesised in four batches of 0.025 g mass each, by adding a known weight of silica gel to titania following a well-defined ratio of TiO_2/silica gel: 100/0 (Ti); 80/20 (Ti80), 50/50 (Ti50) and 20/80 (Ti20). The samples were ground for 2 min in an agate mortar.

2.3. Physical characterization

The determination of the mineralogical composition of the silica gels and commercial titania (Aeroxide P25, Evonik, Aveiro, Portugal) was carried out using a Panalytical X'Pert PRO X-ray diffractometer (Geobiotec, Geosciences Dept, University of Aveiro, Portugal) (CuKα, λ = 0.154056 nm) [36]. The collected data (10°–80° 2θ range, scan rate of 0.02° (2θ)) were processed by Panalytical X'Pert Highscore software (Geobiotec, Geosciences Dept, University of Aveiro, Portugal). The morphology of the obtained products was characterized by scanning electron microscopy (SEM - Hitachi SU-70, Portugal). The specific surface area (S_{BET}) and porosity of the solids were measured by Brunauer–Emmett–Teller (BET) (FlowPrep 060, Portugal) method based on the adsorption and desorption of nitrogen at 77 K. Sieved fractions below 150 microns were degassed at 70°C under high vacuum for 72 h [37]. The dye used in this work is the MB, a heterocyclic aromatic compound with molecular formula $C_{16}H_{18}N_3SCl$. The dye was supplied by Sigma-Aldrich (Aveiro, Portugal).

2.4. Adsorption experiments

The study of the adsorption kinetics of the cationic dye was performed in batches at room temperature (25°C) by varying the contact time and the initial MB dye concentration (5, 10, 15, 20, and 25 mg/L). 0.01 g of silica gel was added to 400 mL of dye solution (wastewater). Using a mechanical stirrer, the solutions were vigorously mixed in the dark, and samples were taken at several time intervals (0, 5, 10, 20, 40, 60, 90, 120, 180, and 240 min). After each adsorption test, the mixture was separated into two phases (solid and liquid) by centrifugation (4,000 rpm for 15 min). The supernatant containing the dye was analyzed by a PerkinElmer lambda 25 spectrophotometer (Department of Materials and Ceramic Engineering, University of Aveiro, Portugal) by measuring the absorbance at a wavelength of 663 nm.

The MB discoloration rate, disc (%) and uptake, q_e (mg/g), were calculated according to Eqs. (1) and (2), respectively.

$$\text{Disc (\%)} = ((C_i - C_e)/C_i) \times 100 \quad (1)$$

$$q_e = (C_i - C_e)V/W \quad (2)$$

Table 1
Synthesis conditions and physical properties of prepared silica gels

Samples	pH	Molar ratio SiO_2/Na_2O	S_{BET} (m^2/g)	Pore volume (cm^3/g)	Pore diameter (Å)
GM3	3.0	1.5	194	0.53	111
GM6	6.0	1.5	91	0.23	79
GM10	10.0	1.5	33	0.12	129

where C_i is the initial concentration of MB (mg/L), C_e is the concentration of the MB at equilibrium (mg/L), q_e is the adsorbed quantity expressed as mg of solute per gram of adsorbent, V (ml) in the volume of the solute; W (g) is the mass of adsorbent.

The Langmuir and Freundlich models are often used for determining the maximum capacity of the binding of pollutants, and identification of the adsorption type. These two models allowed us to calculate the maximum adsorption capacity, as well as the parameters of adsorption [38].

The Langmuir equation may be expressed as follows:

$$t/q_e = (1/q_m) + 1/(K_L q_m C_e) \quad (3)$$

where q_m (mg/g) is the maximum amount adsorbed, q_e (mg/g) is the amount adsorbed at equilibrium, K_L (L/mg) is the Langmuir constant and $1/K_L$ is the slope of the plot. These two parameters (q_m and K_L) are evaluated, respectively, starting from the intersection with the ordinate at the beginning and the slope of the right-hand side $C_e/q_e = f(C_e)$.

The Freundlich model is described by the following equation (4):

$$\log q_e = \log K_f + (1/n) \log C_e \quad (4)$$

where q_e is the amount of dye in mg absorbed per unit g of absorbent at equilibrium, C_e (mg/L) is the concentration of dye solution at equilibrium, K_f is the Freundlich constant and n is a parameter which represents the absence of linearity of the adsorbed quantity as a function of C_e.

In the case of Langmuir models, to know if favorable or unfavorable adsorption is occurring, a factor of separation R_L is used [14]. This factor is defined by the following relation [39]:

$$R_L = 1/1 + K_L C_0 \quad (5)$$

where K_L is the Langmuir constant (l mg^{-1}) and C_0 is the initial concentration of the dye (mg L^{-1}).

The adsorption kinetics was evaluated following pseudo-first and second-order equations.

The pseudo-first-order equation [40] is given by:

$$\log (q_e - q_t) = \log q_e - (k_1/2.303)t \quad (6)$$

where q_e (mg/g) is the capacity at adsorption equilibrium, q_t (mg/g) is the quantity of adsorbent at the time t (min) and k_1 is the equilibrium rate constant (min^{-1}).

The pseudo-second-order kinetics may be expressed as [40]:

$$t/q_t = 1/k_2 q_e^2 + t/q_e \quad (7)$$

where q_e (mg/g) is the capacity at adsorption equilibrium, and k_2 (g mol^{-1} min^{-1}) is the constant speed of adsorption.

2.5. Photocatalytic experiments

The photocatalytic effect of the TiO_2/silica gel composites was studied by testing the degradation of MB at room temperature. 0.005 g of photocatalyst was suspended in 400 mL of 10 mg/L MB solution in a beaker. In the preliminary experiments, reactants were premixed in the dark for 30 min to allow adsorption. After that, UV germicidal lamps (Philips PL-S 9W, NL) (Geobiotec, Geosciences Dept, University of Aveiro, Portugal) were switched on to initiate the photocatalytic decoloration reaction. UV irradiance was a 13 W m^{-2}. At an interval of 1 h, 15 mL samples were drawn out of the reactor to determine the change of the MB concentration, by measuring the absorbance on a UV-Vis spectrometer (PerkinElmer lambda 25) (Department of Materials and Ceramic Engineering, University of Aveiro, Portugal). The photocatalytic decoloration efficiency ξ (%) was measured as:

$$\xi\ (\%) = ((C_0 - C_s)/C_0) \times 100 \quad (8)$$

where C_0 is the initial concentration for the calculation of the photocatalytic decoloration efficiency ($C_0 = (C_i - C_e)$) and C_s is the concentration of the MB at the specific reaction time (mg/L).

The apparent speed constant (k'_{app}) was measured by the pseudo-first-order reaction as follows:

$$\ln (C_0/C) = k'_{app}\, t \quad (9)$$

where C_0 and C are the initial concentration for the calculation of the photocatalytic decoloration efficiency (mg/L) at 0 min and after a certain irradiation time t (min), respectively. The plot of ln (C_0/C) vs. the contact time t under UV exposure, gives a straight line, whose slope indicates the value of the pseudo-first-order apparent rate constant (k'_{app}) [14,41].

3. Results and discussion

3.1. Characterization of silica gels and silica gel/TiO_2

According to the X-ray diffraction (XRD) diagrams obtained (Fig. 1), the silica gel has a mineralogical composition virtually identical irrespective of pH of synthesis (Fig. 1a). They are characterized by a large amorphous hump centered at around 2θ = 23°, indicating their accentuated amorphous nature, with crystalline peaks of quartz, and in the case of GM10, a very small amount of poorly crystalline feldspar. The XRD patterns of pure TiO_2 are shown in Fig. 1b and the TiO_2 P25 powder consists of mostly anatase, with some secondary rutile phase.

Fig. 2 shows SEM images of silica gel GM3 and the silica gel/titania composite (GM3)/TiO_2 (20/80). The silica gels (Fig. 2a) present similar structures with large particle aggregates of 1.14 to 5.45 μm. Almost the same results were found by Brahmi et al. [33] for the size of silica gel prepared from Algerian siliceous sands. The SEM image (Fig. 2b) of the silica gel/TiO_2 composite showed that TiO_2 nanoparticles were well immobilized on the adsorbent; some of them were agglomerated on the surface of the adsorbent.

The BET specific surface area (SSA) of the silica gels are reported in Table 1. The values of the SSA of products prepared at pH 3, pH 6, and pH 10 were 194, 91, and 33 m^2/g, respectively. Hence, silica gel was prepared at pH 3 (GM3) had a higher surface area compared with the silica gel were synthesized at pH 6 (GM6) and pH 10 (GM10). These results

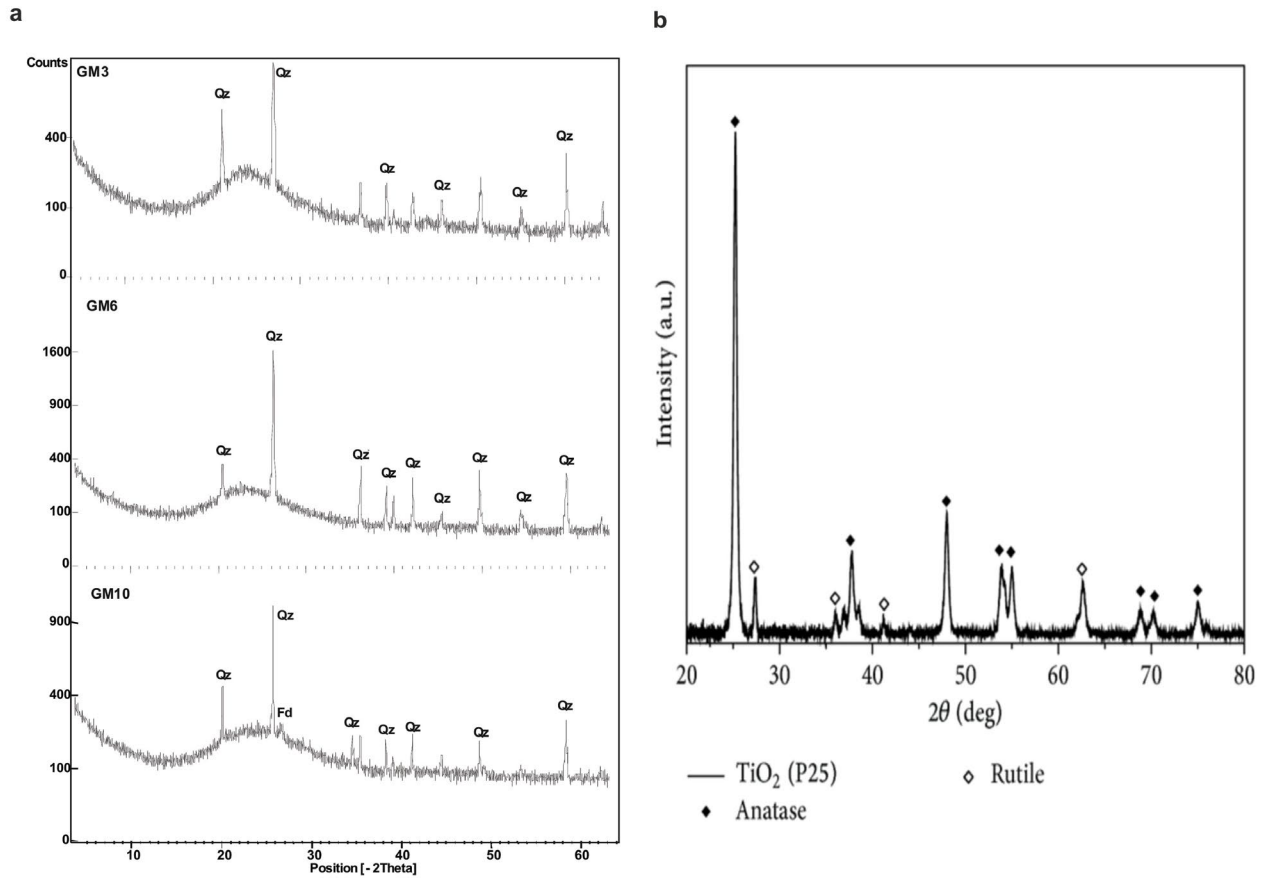

Fig. 1. X-ray diffractogram of (a) silica gel: Qz, quartz and Fd, Feldspar; (b) TiO_2 P25.

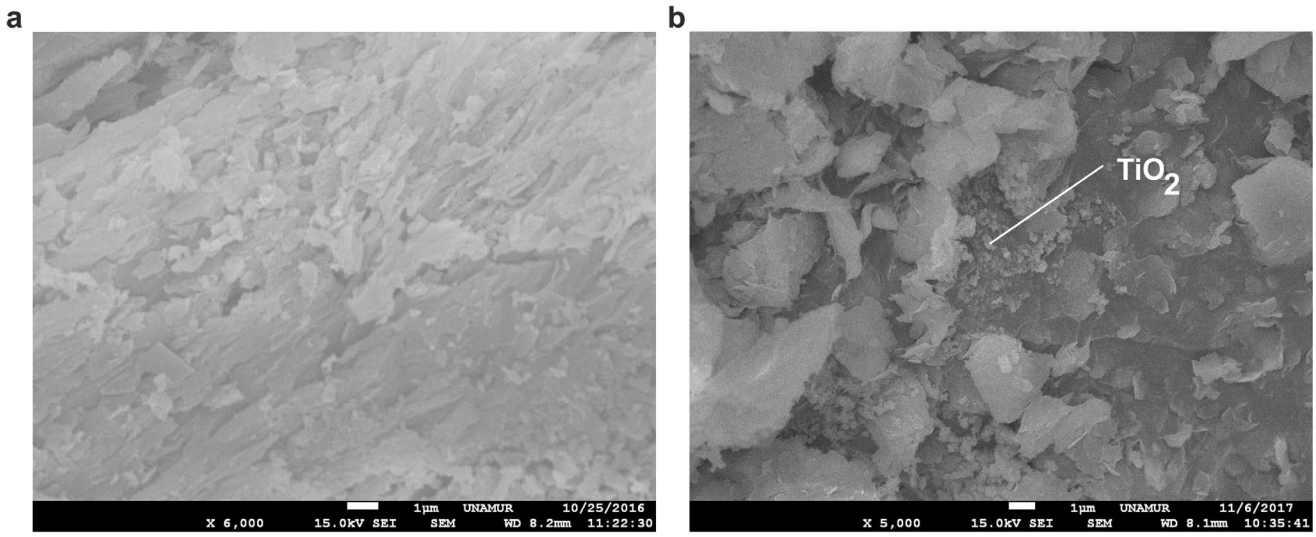

Fig. 2. SEM images of (a) silica gel (GM3) and (b) silica gel (GM3)/TiO_2 (Ti80).

are a good agreement with previous results in the literature [42]. The nitrogen adsorption–desorption isotherms of the silica gels are shown in Fig. 3, and they have a type II adsorption isotherm. They present pore volumes varying from 0.12 to 0.53 cm^3/g (Table 1) and pore diameters ranging from 79 to 129 Å, the largest values being for GM3, this indicates that our silica gel is a mesoporous material, with the pore diameter exceeding 20 Å [43].

3.2. Adsorption experiments

3.2.1. MB adsorption performance

The effect of pH on the adsorption of synthesis onto silica gels (pH 3, 6, and 10) is shown in Fig. 4. The results obtained show that the time required for equilibrium is reached after 240 min reaction time, but that the adsorption begins to plateau after 120 min. The removal efficiency for GM3 exceeded 81% after 240 min, compared to 66% and 49% for GM6 and GM10. Therefore, the retention of MB by the silica gel is favorable when synthesized at acid pH (pH 3), and decreases when synthesized at pH 6 and 10. As GM3 showed superior MB adsorption, this silica gel was used for subsequent experiments.

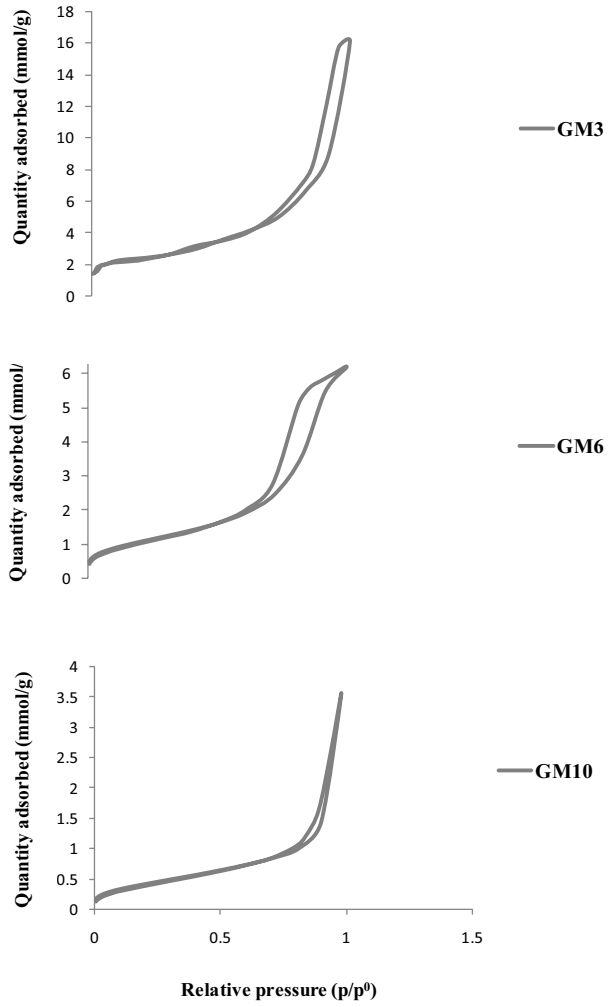

Fig. 3. Nitrogen adsorption isotherms for silica gels.

The increased surface area of GM3 will have an effect on this adsorption. However, the influence of synthesis pH on the adsorption of MB may also partly be due to the surface charge of the adsorbents [5,44,45].

Fig. 5 shows the effect of GM3 of varying the initial concentration of MB (5–25 mg/L) on the adsorption. The results show that the MB adsorption capacity increases with the decrease in the initial concentration of dye, as would be expected. The adsorption rate of the GM3 exceeded 91% even after 180 min reaction time using just 5 mg/L (Fig. 5). When this initial concentration dye was elevated to 25 mg/L, the adsorption rate of the adsorbent GM3 decreased to 41%, due to the saturation of the active sites in the adsorbent [5,46]. Even if the adsorption is supposed to follow a multilayer mechanism, at high concentrations of dye greater competition between the MB molecules occurs.

3.2.2. Equilibrium and kinetics of MB adsorption

The calculated Langmuir and Freundlich parameters are presented in Fig. 6 and Table 2. The experimental data fit better with the Langmuir adsorption isotherm model, as the values of coefficients of determination (R^2) are closer to 1

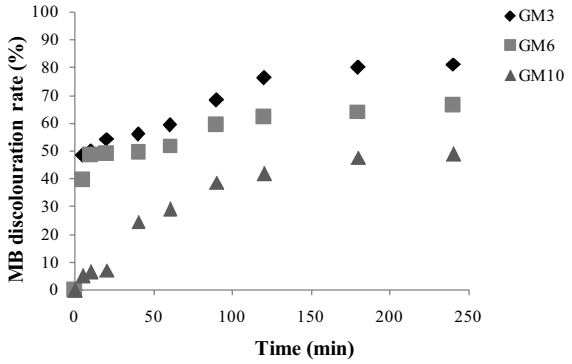

Fig. 4. Adsorption kinetics: effect of pH of silica gel synthesis on subsequent adsorption of MB. Experimental conditions: C_i, 10 ppm; T, 25°C; pH, 3; 6 and 10; $m_{adsorbent}$, 0.01 g.

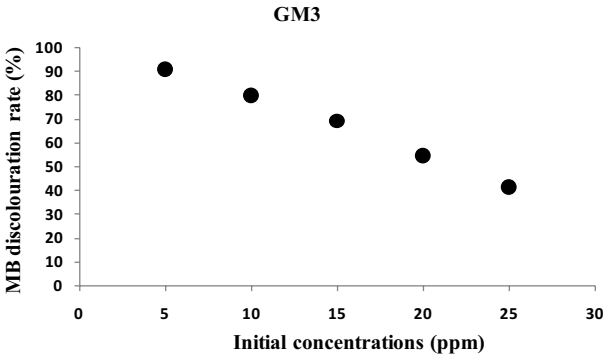

Fig. 5. Adsorption kinetics: effect of initial concentration of MB in dye solution on adsorption of MB. Experimental conditions: T, 25°C; synthesis pH, 3; $m_{adsorbent}$, 0.01 g; time of equilibrium, 180 min.

(Fig. 6a), indicating that the adsorption process corresponds to monolayer coverage of MB molecules over the surface of the samples analyzed. The results indicated that higher adsorption capacity (q_m) was achieved by GM3 (125 mg/g) (Table 2) compared to those obtained by GM6 (91 mg/g) and GM10 (74 mg/g), GM3 also having the higher SSA. Our results indicated that R_L ranged between 0 and 1 for the adsorption of MB on GM3, indicating favorable adsorption.

For the Freundlich model, the measured parameters are summarised in Table 2 and Fig. 6b. A lower affinity for interaction between the adsorbate–adsorbent was revealed by the smaller R^2 regression coefficient. The above fact shows a monolayer adsorption with a heterogeneous energetic distribution of active sites, accompanied by interactions between the adsorbed molecules.

The parameters calculated for the various kinetic models (pseudo-first-order and pseudo-second-order) are presented in Figs. 6c and d. A much better fit (R^2 = 0.99) was described by the pseudo-second-order model. Moreover, the calculated adsorption capacity at equilibrium ($q_{e,cal}$) is very close

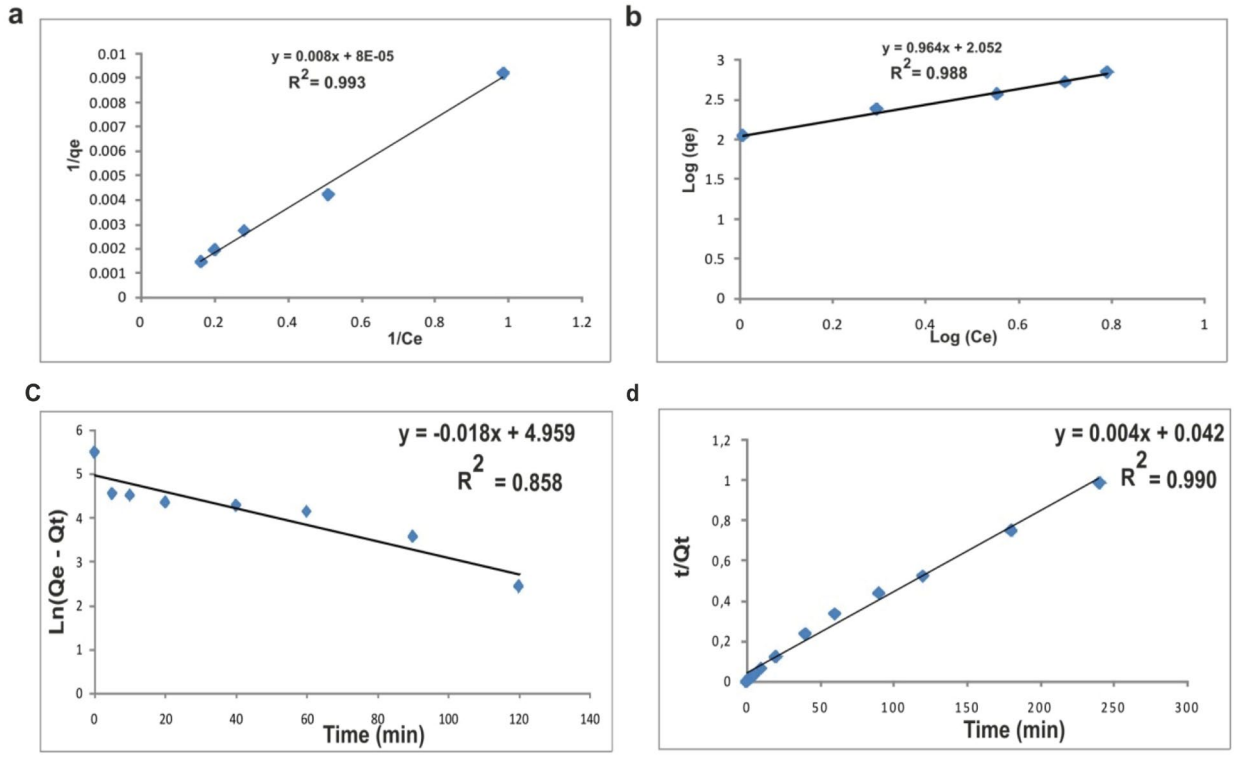

Fig. 6. Fitting with the linear Langmuir (a) and Freundlich (b) models for MB adsorption on GM3. Experimental conditions: C_i, 10 ppm; T, 25°C; synthesis pH, 3; $m_{adsorbent}$, 0.01 g; time, 180 min. Kinetics by the pseudo-first-order (c) and pseudo-second-order (d) models for MB adsorption on GM3.

Table 2
Langmuir and Freundlich parameters for MB adsorption

	Langmuir				Freundlich		
Material	q_m (mg/g)	K_L (L/mg)	R_L	R^2	K_f (L/g)	n	R^2
GM3	125	1,000	0.00091	0.993	112.72	1.03	0.988

Table 3
Pseudo-first and second-order parameters for MB adsorption

	Pseudo-first-order				Pseudo-second-order		
Material	k_1 (min^{-1})	q_e (mg/g)	R^2	q_e (exp)	k_2 (g/mg min)	q_e (mg/g)	R^2
GM3	–0.018	142.4	0.858	239.6	0.00038	250.0	0.990

Table 4
Photocatalytic decoloration efficiency (ξ), and correlation coefficient (R^2) of the pseudo-first-order apparent constant of the photocatalytic reaction (Ti = 100% TiO_2)

	R^2				ξ(%)			
Material	Ti	Ti80	Ti50	Ti20	Ti	Ti80	Ti50	Ti20
GM3	0.97	0.93	0.87	0.74	99	93	91	88
GM6	0.97	0.90	0.85	0.71	99	83	79	73
GM10	0.97	0.89	0.83	0.67	99	76	72	67

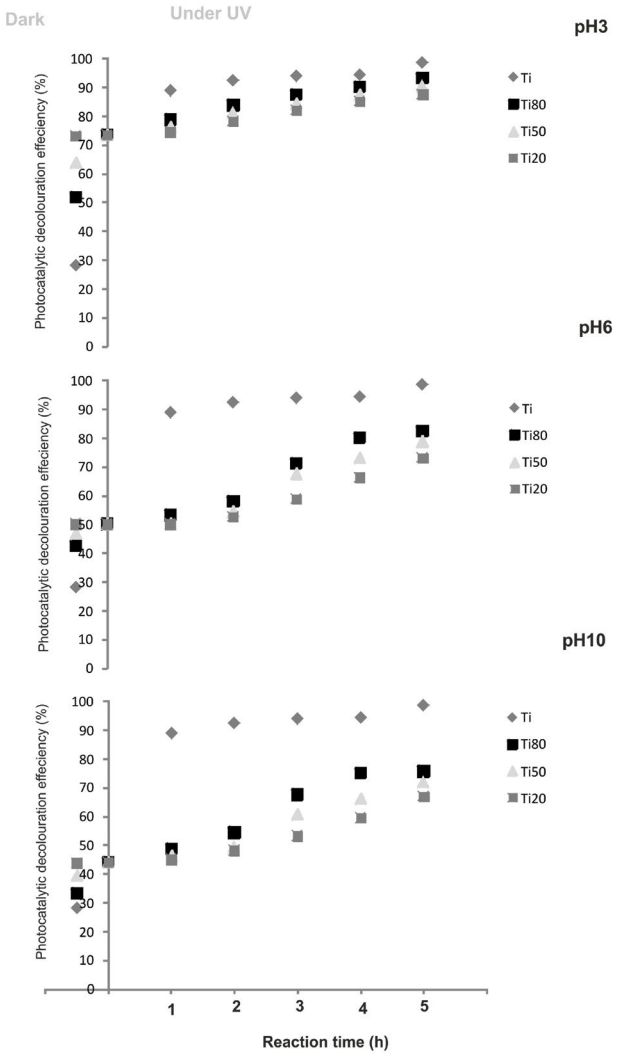

Fig. 7. Photocatalytic removal kinetics of MB dyes under UV light by GM based titania/silica gel composites synthesis at pH 3, 6 and 10.

to the value obtained experimentally ($q_{e,cal}$) (Table 3). Thus, the adsorption of MB on silica gel might be explained by the pseudo-second-order kinetic model. These results suggest a chemisorption mechanism, involving covalent forces through the sharing or exchange of electrons between sorbent and sorbate.

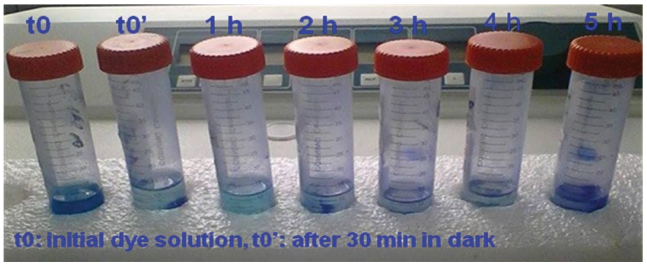

Fig. 8. Photo-induced decoloration of dye solution (MB) by the silica gel/titania P25 composites as a function of time.

3.3. Photocatalytic decoloration of MB

3.3.1. Photocatalytic decoloration efficiency

The silica gel/titania P25 can have the added photocatalytic properties from titania P25, the high stability from silica gel and extra properties coming from chemical bonds between two composites. Table 4, Figs. 7 and 8 show the results of photo-induced removal of cationic MB dye solution (10 mg/L) by GM3, GM6 and GM10 silica gel/titania P25 composites, having different proportions of TiO_2. In darkness, the adsorption of MB on the silica gel/TiO_2 increased with increasing the proportion of silica gel (Fig. 7). This explains the lowest photodecolouration correlation coefficient R^2 observed in Ti20 samples (Table 2). Under UV irradiation (after 5 h of reaction), the MB decolouration of pure P25 titania (99%) is slightly superior to that of the silica gel (GM3)/TiO_2 composites (Ti80 (93%), Ti50 (91%), and Ti20 (88%)) (Fig. 7), as they have less titania present, although they have broadly similar. However, one advantage of dispersion of TiO_2 nanoparticles onto the adsorbent gel is that it gives a good adherence between the support and the catalyst over a sustained period, without adversely affecting its photocatalytic [15,47].

The results indicate that the synthesized photocatalyst can effectively degrade the MB. The photocatalytic activity of silica gel samples was increased by the increase in TiO_2 loading. Fig. 7 also indicates that the photocatalytic activity of pure TiO_2 P25 is higher than that of the silica gel/TiO_2 samples. This result could be due to the poor accessibility to the TiO_2 P25 surface. However, the silica gel/TiO_2 P25 samples can be readily separated from the suspension after the reaction because they sediment in minutes when the stirring was stopped, while the TiO_2 sample could not sediment easily, and lead to potential difficulty in downstream separation.

Table 5
Apparent constant of the photocatalytic reaction rate as a function of the percentage of TiO_2

TiO_2 (%)	k'_{app} (min^{-1})
100	0.406
80	0.269
50	0.236
20	0.158

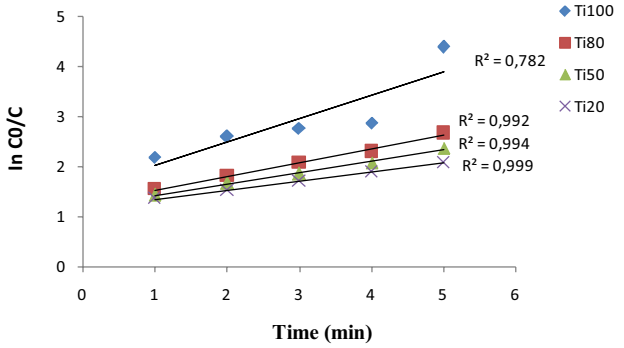

Fig. 9. Photocatalytic rate constants as a function of the different amounts of TiO_2/silica gel (GM3).

With the combined effects of adsorption and photocatalysis, very satisfactory decoloring efficiency was achieved with mixtures, even those containing low TiO_2 amounts. The samples GM6 and GM10 based composites show lower decoloring performance (ξ equal to 73 and 67% for GM6 and GM10, respectively; Table 4), and this could be related to the inferior SSA of the silica gel.

3.3.2. Kinetics of MB decoloration

Adsorption tests in the dark were carried out to evaluate the adsorbed quantities of MB on the photocatalyst surface. Fig. 7 indicates that the adsorbed quantities do not exceed 73% of the initial quantity in the solution. The adsorbed quantities of MB decrease with the augmentation of TiO_2 content. This result can be explained by the availability of more adsorption sites at the surface of the composite silica gel/TiO_2.

The plot of $\ln(C_0/C)$ vs. t with different amounts of silica gel (GM3)/TiO_2 is shown in Table 5 and Fig. 9. All the curves showed a good linear correlation ($R^2 > 0.99$ for silica gel/TiO_2), suggesting that the decoloration of MB by silica gel-TiO_2/UV followed a first-order kinetic.

Under the same experimental conditions, the apparent rate constant (k'_{app}) of MB decoloration was 0.406, 0.269, 0.236, and 0.158 min^{-1}, while the percentage (%) of TiO_2 was 100, 80, 50, and 20, respectively. As the mass of TiO_2 (100%) increases, the apparent rate constant increases.

3.4. Mechanism of MB decoloration process

For MB adsorption, it was clear that silica gel GM3 shows the highest adsorption capacity (81%) due to the larger surface area. The adsorption capacity of these silica gel materials increased to 83% when reducing the concentration MB to 5 ppm. The percentage of decoloration was influenced by the change in pH. The discoloration of the dye was upgraded to 49% for the GM at pH 10. The isotherms of the adsorption of the MB dye on silica gel by the Langmuir isotherm model parameters were very favorable (R^2 up to 0.99), and this reveals that the adsorption process corresponds to monolayer coverage of MB molecules over the surface of the silica gel samples.

With the combined effects of adsorption and photocatalytic decoloration, very satisfactory decoloring efficiency was presented with mixtures, even those containing low TiO_2 quantity. Silica gel/TiO_2 composites at basic pH show lower decoloring performance (ξ equal to 67%), and this could be related to the inferior SSA of the silica gel.

4. Conclusions

In this work, it has been studied the used to a local natural Tunisian sand for the preparation of silica gels and their potential retention of a cationic dye (MB).

Based on the results obtained, the following conclusions can be drawn:

- For MB adsorption, it was clear that silica gel GM3 shows the highest adsorption capacity (81%).
- The absorption efficiency of these silica gel materials increased to 83% when reducing the concentration MB to 5 mg/L.
- The isotherms of the adsorption of the MB dye on silica gel by the Langmuir isotherm model parameters were very favorable (R^2 up to 0.99).
- The pseudo-second-order expression (R^2 equals to 0.99) is better fitted to describe the adsorption kinetics of analyzed samples.
- The used of mixtures made by different reports of silica gel/P25 TiO_2, prepared to ensure photocatalytic properties. The high photocatalytic decoloration rate of MB of silica gel/TiO_2 composite (even with a mixture containing low TiO_2 contents) is attributed to the excellent adsorption effect in the dark and high-efficiency photocatalytic decoloration (99% removal after 300 min) in the presence of UV light irradiation at acidic pH.
- The results were found that these photocatalysts can effectively degrade the MB.
- The high photodegradation of MB by silica gel/TiO_2 is due to the anatase phase stability of the used photocatalyst.
- A kinetic study was performed and showed that the discoloration of dyes followed a pseudo-first-order rate law.
- This study demonstrated the applicability of silica gel/TiO_2 P25 for catalytic treatment of MB.

Acknowledgments

This work was supported by FCT grant SFRH/BPD/72398/2010 and by UID/GEO/04035/2013 project. This study was supported by funding from MEDYNA: "FP7-Marie Curie Action funded under Grant Agreement PIRSES-GA-2013-612572", and the Tunisian Belgium Wallonie-Bruxelles International WBI Research Project "Valorisation des Argiles tunisiennes". Robert C. Pullar acknowledges the support

of the Fundação para a Ciência e Tecnologia (FCT) grant IF/00681/2015, and this work was developed within the scope of the FCT project CICECO-Aveiro Institute of Materials (FCT UID/CTM/50011/2019), financed by national funds through the FCT/MCTES.

References

[1] P.A. Carneiro, R.F.P. Nogueira, M.V.B. Zanoni, Homogeneous photodegradation of C.I. reactive blue 4 using a photo – Fenton process under artificial and solar irradiation, Dyes Pigm., 74 (2007) 127–132.
[2] J.E.B. McCallum, S.A. Madison, S. Alkan, R.L. Depinto, R.U.R. Wahl, Analytical studies on the oxidative degradation of the reactive textile dye Uniblue A, Environ. Sci. Technol., 34 (2000) 5157–5164.
[3] Y.D. Sintayehu, A.B. Gemeta, S.G. Berehe, Optical photocatalytic degradation of methylene blue using lignocellulose modified TiO_2, Int. J. Photochem. Photobiol., 2 (2017) 81–84.
[4] A. Arunkumar, T. Chandrasekaran, K.R. Ahamed, ZnO doped with activated carbon for photocatalytic degradation of methylene blue and malachite green on UV–visible light, Int. J. Nano Corros. Sci. Eng., 2 (2015) 300–307.
[5] K. Lazaar, W. Hajjaji, R.C. Pullar, J.A. Labrincha, F. Rocha, F. Jamoussi, Production of silica gel from Tunisian sands and its adsorptive properties, J. Afr. Earth. Sci., 130 (2017) 238–251.
[6] I. Koyuncu, Reactive dye removal in dye/salt mixtures by nanofiltration membranes containing vinylsulphone dyes: effects of feed concentration and cross flow velocity, Desalination, 143 (2002) 243–253.
[7] X. Jiang, K. Cai, J. Zhang, Y. Shen, S.G. Wang, X.Z. Tian, Synthesis of a novel water-soluble chitosan derivative for flocculated decolorization, J. Hazard. Mater., 185 (2011) 1482–1488.
[8] Ö. Gök, A.S. Özcan, A. Adnan, Adsorption behavior of a textile dye of reactive blue 19 from aqueous solutions onto modified bentonite, Appl. Surf. Sci., 256 (2010) 5439–5443.
[9] G. Moussavi, M. Mahmoudi, Removal of azo and anthraquinone reactive dyes from industrial wastewaters using MgO nanoparticles, J. Hazard. Mater., 168 (2009) 806–812.
[10] M.H. Do, N.H. Phan, T.D. Nguyen, T.T.S. Pham, V.K. Nguyen, T.T.T. Vu, T.K.P. Nguyen, Activated carbon/Fe_3O_4 nanoparticle composite: fabrication, methyl orange removal and regeneration by hydrogen peroxide, Chemosphere, 85 (2011) 1269–1276.
[11] G. Xue, H.H. Liu, Q.Y. Chen, C. Hills, M. Tyrer, F. Innocent, Synergy between surface adsorption and photocatalysis during degradation of humic acid on TiO_2/activated carbon composites, J. Hazard. Mater., 186 (2011) 765–772.
[12] J.R. Guimarães, M.G. Maniero, R. Nogueira de Araújo, A comparative study on the degradation of RB-19 dye in an aqueous medium by advanced oxidation processes, J. Environ. Manage., 110 (2012) 33–39.
[13] J.G. Qu, N.N. Li, B.J. Liu, J.X. He, Preparation of $BiVO_4$/bentonite catalysts and their photocatalytic properties under simulated solar irradiation, Mater. Sci. Semicond. Process., 16 (2013) 99–105.
[14] W. Hajjaji, S.O. Ganiyu, D.M. Tobaldi, S. Andrejkovičová, R.C. Pullar, F. Rocha, J.A. Labrincha, Natural Portuguese clayey materials and derived TiO_2-containing composites used for decolouring methylene blue (MB) and orange II (OII) solutions, Appl. Clay Sci., 83 (2013) 91–98.
[15] B.L. Xing, C.L. Shi, C.X. Zhang, G.Y. Yi, L.J. Chen, H. Guo, G.X. Huang, J.L. Cao, Preparation of TiO_2/activated carbon composites for photocatalytic degradation of RhB under UV light irradiation, J. Nanomater., 2016 (2016) 10 p, doi: org/10.1155/2016/8393648.
[16] J. Araña, J.M. Doña-Rodríguez, E.T. Rendón, C. Garriga i Cabo, O. González-Díaz, J.A. Herrera-Melián, J.M. Pérez-Peña, G. Colón, J.A. Navío, TiO_2 activation by using activated carbon as a support: Part I. Surface characterisation and decantability study, Appl. Catal., B, 44 (2003) 161–172.
[17] Z. Zainal, L.K. Hui, M.Z. Hussein, A.H. Abdullah, Imad (Moh'd Khair) Rashid Hamadneh, Characterization of TiO_2–chitosan/glass photocatalyst for the removal of a monoazo dye via photodegradation–adsorption process, J. Hazard. Mater., 164 (2009) 138–145.
[18] T. Kodom, G. Djaneye-Boundjou, L.M. Bawa, B. Gombert, N. Alonso-Vante, Etude de la photodégradation du reactive black 5 et du reactive orange 16 en solution aqueuse en utilisant des couches minces de TiO_2, Int. J. Biol. Chem. Sci., 5 (2011) 232–246.
[19] W.L.F. Armarego, C.L.L. Chai, Purification of Laboratory Chemicals, 7th ed., Butterworth-Heinemann is an imprint of Elsevier, Australian National University, Canberra A.C.T., Australia, 2013.
[20] J.M. Gómez, J. Galán, A. Rodríguez, G.M. Walker, Dye adsorption onto mesoporous materials: pH influence, kinetics and equilibrium in buffered and saline media, J. Environ. Manage., 146 (2014) 355–361.
[21] J. Lin, H.Y. Zhang, H.Q. Hong, H. Liu, X.B. Zhang, A Thermally conductive composite with a silica gel matrix and carbon-encapsulated copper nanoparticles as filler, J. Electron. Mater., 43 (2014) 2759–2769.
[22] Y. Liu, J. Shen, B. Zhou, G.M. Wu, Z.H. Zhang, Effect of hydrophobicity on the stability of sol–gel silica coatings in vacuum and their laser damage threshold, J. Sol-Gel Sci. Technol., 68 (2013) 81–87.
[23] D. Château, Etude de l'influence de la structure et de la composition de matériaux hybrides monolithiques sur les propriétés optiques (luminescence et absorption non-linèaire), Thèse de doctorat, Ecole normale supérieure de Lyon, France, 2013, p. 138.
[24] Q. Xu, P. Yin, G.F. Zhao, G. Yin, R.J. Qu, Synthesis and characterization of silica gel microspheres encapsulated by salicyclic acid functionalized polystyrene and its adsorption of transition metal ions from aqueous solutions, Cent. Eur. J. Chem., 8 (2010) 214–222.
[25] A. Brown, M. Augustin, M. Jünger, M. Zutt, J. Dissemond, E. Rabe, R. Kaufmann, M. Simon, M. Stücker, S. Karrer, W. Koenen, W. Vanscheidt, K. Scharfetter-Kochanek, U. Wollina, T. Krieg, S.A. Eming, Randomized standard-of-care-controlled trial of a silica gel fibre matrix in the treatment of chronic venous leg ulcers, Eur. J. Dermatol., 24 (2014) 210–216.
[26] X.T. Gao, I.E. Wachs, Titania–silica as catalysts: molecular structural characteristics and physico-chemical properties, Catal. Today, 51 (1999) 233–254.
[27] Y.M. Wang, S.W. Liu, Z.L. Xiu, X.B. Jiao, X.P. Cui, J. Pan, Preparation and photocatalytic properties of silica gel-supported TiO_2, Mater. Lett., 60 (2005) 974–978.
[28] E.M. de la Fournière, A.G. Leyva, E.A. Gautier, M.I. Litter, Treatment of phenylmercury salts by heterogeneous photocatalysis over TiO_2, Chemosphere, 67 (2007) 682–688.
[29] V. Matějka, P. Matějková, P. Kovář, J. Vlček, J. Přikryl, P. Červenka, Z. Lacný, J. Kukutschová, Metakaolinite/TiO_2 composite: photoactive admixture for building materials based on Portland cement binder, Constr. Build. Mater., 35 (2012) 38–44.
[30] Y. Hendrix, A. Lazaro, Q.L. Yu, J. Brouwers, Titania-silica composites: a review on the photocatalytic activity and synthesis methods, World J. Nano Sci. Eng., 5 (2015) 161–177.
[31] R. De-Richter, S. Caillol, Fighting global warming: the potential of photocatalysis against CO_2, CH_4, N_2O, CFCs, tropospheric O_3, BC and other major contributors to climate change, J. Photochem. Photobiol., 12 (2011) 1–19.
[32] W. Trabelsi, M. Benzina, S. Bouaziz, Physico-chemical characterisation of the Douiret sand (Southern Tunisia): valorisation for the production of silica gel, Physics Procedia, 2 (2009) 1461–1467.
[33] D. Brahmi, D. Merabet, H. Belkacemi, T.A. Mostefaoui, N. Ait Ouakli, Preparation of amorphous silica gel from Algerian siliceous by-product of kaolin and its physico chemical properties, Ceram. Int., 40 (2014) 10499–10503.
[34] A. Radian, K.G. Aukema, A. Aksan, L.P. Wackett, Silica gel for enhanced activity and hypochlorite protection of cyanuric acid hydrolase in recombinant Escherichia coli, Am. Soc. Microbiol., 6 (2015) e1477–15.

[35] S. Marzouk, F. Rachdi, M. Fourati, J. Bouaziz, Synthesis and grafting of silica aerogels, Colloids Surf., A, 234 (2004) 109–116.
[36] R.M. Ali, H.A. Hamad, M.M. Hussein, G.F. Malash, Potential of using green adsorbent of heavy metal removal from aqueous solutions: adsorption kinetics, isotherm, thermodynamic, mechanism and economic analysis, Ecol. Eng., 91 (2016) 317–332.
[37] S. Brunauer, P.H. Emmett, E. Teller, Adsorption of gases in multimolecular layers, J. Am. Chem. Soc., 60 (1938) 309–319.
[38] Z. Meçabih, S. Kacimi, B. Bouchikhi, Adsorption des matières organiques des eaux usées urbaines sur la bentonite modifiée par Fe(III), Al(III) et Cu(II), Rev. Sci. Eau/J. Water Sci., 19 (2006) 23–31.
[39] D. Ašperger, I. Varga, S. Babić, L. Ćurković, Adsorption of enrofloxacine on natural zeolite – clinoptilolite, Holistic Approach Environ., 4 (2014) 3–15.
[40] A. Robalds, L. Dreijalte, O. Bikovens, M. Klavins, A novel peat-based biosorbent for the removal of phosphate from synthetic and real wastewater and possible utilization of spent sorbent in land application, Desal. Wat. Treat., 57 (2016) 13285–13294.
[41] H. Al-Ekabi, N. Serpone, Kinetics studies in heterogeneous photocatalysis. I. Photocatalytic degradation of chlorinated phenols in aerated aqueous solutions over titania supported on a glass matrix, J. Phys. Chem., 92 (1988) 5726–5731.
[42] M. Prassas, Synthese des gels du système SiO_2–Na_2O et des gels monolithiques de silice, Etude de leur conversion en verre, Thèse de Doctorat, Montpellier, France, 1981.
[43] P. Webb, C. Orr, Analytical Methods in Fine Particle Technology, Micromeritics Instrument Corporation, Norcross, GA, 1988.
[44] F. Sakr, A. Sennaoui, M. Elouardi, M. Tamimi, A. Assabbane, Étude de l'adsorption du Bleu de Méthylène sur unbiomatériau à base de Cactus (Adsorption study of Methylene Blue on biomaterial using cactus), J. Mater. Environ. Sci., 6 (2015) 397–406.
[45] A. Boukraa, F. Messemmeche, Etude qualitative et quantitative de l'adsorption de bleu de méthylène sur le charbon actif en poudre, Revue science des matériaux, 7 (2016) 25–41.
[46] E. Errais, J. Duplay, F. Darragi, I. M'Rabet, A. Aubert, F. Huber, G. Morvan, Efficient anionic dye adsorption on natural untreated clay: kinetic study and thermodynamic parameters, Desalination, 275 (2011) 74–81.
[47] Z. Huang, P. Wu, Y. Lu, X. Wang, N. Zhu, Z. Dang, Enhancement of photocatalytic degradation of dimethyl phthalate with nano-TiO_2 immobilized onto hydrophobic layered double hydroxides: a mechanism study, J. Hazard. Mater., 70 (2013) 246–247.